Synergetic Ferroelectricity and Superconductivity in Zero-Density Dirac Semimetals near Quantum Criticality

Vladyslav Kozii,[1,2,3] Avraham Klein,[4,5] Rafael M. Fernandes,[5] and Jonathan Ruhman[6,7]
[1]Department of Physics, Carnegie Mellon University, Pittsburgh, Pennsylvania 15213, USA
[2]Department of Physics, University of California, Berkeley, California 94720, USA
[3]Materials Sciences Division, Lawrence Berkeley National Laboratory, Berkeley, California 94720, USA
[4]Physics Department, Ariel University, Ariel 40700, Israel
[5]School of Physics and Astronomy, University of Minnesota, Minneapolis, Minnesota 55455, USA
[6]Department of Physics, Bar-Ilan University, 52900 Ramat Gan, Israel
[7]Center for Quantum Entanglement Science and Technology, Bar-Ilan University, 52900 Ramat Gan, Israel

(Received 19 October 2021; revised 5 February 2022; accepted 31 October 2022; published 29 November 2022)

We study superconductivity in a three-dimensional zero-density Dirac semimetal in proximity to a ferroelectric quantum critical point. We find that the interplay of criticality, inversion-symmetry breaking, and Dirac dispersion gives rise to a robust superconducting state at the charge-neutrality point, where no Fermi surface is present. Using Eliashberg theory, we show that the ferroelectric quantum critical point is unstable against the formation of a ferroelectric density wave (FDW), whose fluctuations, in turn, lead to a first-order superconducting transition. Surprisingly, long-range superconducting and FDW orders are found to cooperate with each other, in contrast to the more usual scenario of phase competition. Therefore, we suggest that driving charge neutral Dirac materials, e.g., $Pb_xSn_{1-x}Te$, through a ferroelectric quantum critical point may lead to superconductivity intertwined with FDW order.

DOI: 10.1103/PhysRevLett.129.237001

Introduction.—Superconductivity (SC) is observed in numerous doped materials with extremely low density of free charge carriers. Examples include doped $SrTiO_3$ [1–3], Sr-doped Bi_2Se_3 [4], YPtBi [5], Tl-doped PbTe [6], and elemental bismuth [7]. The observation of low-density SC is surprising for two main reasons [8,9]. First, because the Fermi and the Debye energies are similar in magnitude and therefore the Coulomb repulsion is naively unscreened. Second, the density of states of a three-dimensional Fermi liquid, which affects the transition temperature drastically in conventional superconductors, is orders of magnitude smaller than in standard superconducting alloys. Therefore, finding microscopic models with superconducting instabilities at arbitrarily low density is an outstanding challenge.

A necessary ingredient for realizing low-density SC is a sufficiently long-ranged attractive interaction [10–12]. Such an interaction can be provided by the fluctuations of a bosonic order parameter in the vicinity of a quantum critical point (QCP) [13–16]. In particular, it was proposed that superconductivity in some low-density SCs, such as doped $SrTiO_3$ and $Pb_xSn_{1-x}Te$, originates from the proximity to a ferroelectric (FE) QCP [12,17–25]. Indeed, experiments find that the electronic properties of $SrTiO_3$ are strongly influenced by the transition [23,25–31] and possibly also of $Pb_xSn_{1-x}Te$ [32].

The soft modes near the critical point in polar crystals are transverse. According to the standard description of the electron-phonon interaction, transverse phonons are decoupled from the itinerant electron's density [19,33]. Several mechanisms have been proposed to circumvent this issue, such as coupling to gapped longitudinal modes [19,25], two transverse phonon exchange [34–38], and a linear vector coupling in multiorbital systems [8,12,39–45]. A renormalization group (RG) analysis found the vector coupling is marginally relevant in Dirac semimetals [8]. Based on this observation, it was shown that FE critical fluctuations are a promising pairing mechanism for low-density SC. However, close enough to the QCP these arguments break down since the system flows to strong coupling.

In this Letter, we investigate the fate of the clean ferroelectric QCP in 3D polar Dirac materials at zero density using both Eliashberg and BCS theories. We are deliberately studying this idealized model as a paradigmatic example of a low-density system with strong spin-orbital effects where sharp conclusions can be made. First, we show that the original FE QCP is preempted by a ferroelectric density wave (FDW) QCP due to the coupling between Dirac fermions and transverse optical phonons. This FDW state breaks translational symmetry in addition to inversion and rotational symmetries. Second, we find that the FDW fluctuations, which are peaked on a spherical surface in momentum space, mediate a much stronger attractive interaction as compared to the fluctuations of the uniform FE order. This attraction leads to a SC instability

which, in turn, softens the FDW fluctuations and enhances the pairing interaction even further. Consequently, because of this feedback effect, the system undergoes a first-order transition into a zero-density superconductor coexisting with ferroelectricity of some sort (finite momentum or uniform), before the putative FDW QCP is reached. Thus, in addition to obtaining a zero-density pairing instability, we find an effective *attraction* between FDW and SC order parameters, in sharp contrast to the usually observed competition between SC and other types of order such as antiferromagnetism, nematicity, or charge density wave [46–50].

Model.—We start with the effective low-energy model for a polar Dirac semimetal near a FE transition derived in Ref. [8]. The direct Coulomb repulsion is strongly screened by the longitudinal optical phonon mode which remains massive at the critical point and does not contribute to the low-energy properties [51]. The massless 3D Dirac fermions $\psi_{\mathbf{k}}$ are then only coupled to the transverse optical phonon mode $\varphi_i(\mathbf{q}) = P_{ij}(\mathbf{q})u_j(\mathbf{q})$, where $u_i(\mathbf{q})$ is proportional to the optical phonon displacement, $P^{ij}(\mathbf{q}) = \delta^{ij} - \hat{q}^i\hat{q}^j$ is the projector onto the transverse modes, and $\hat{\mathbf{q}} \equiv \mathbf{q}/|\mathbf{q}|$. The imaginary-time action of the system is given by $S = \int d\tau(\mathcal{L}_\psi + \mathcal{L}_\varphi + \mathcal{L}_{\psi-\varphi})$, with

$$\begin{aligned}
\mathcal{L}_\psi &= \sum_{n=1}^{N}\sum_{\mathbf{k}} \psi_n^\dagger(\tau,\mathbf{k})(\partial_\tau + iv_F\gamma^j\gamma^0 k_j)\psi_n(\tau,\mathbf{k}),\\
\mathcal{L}_\varphi &= \frac{1}{2}\sum_{\mathbf{q}} \varphi_i^*(\tau,\mathbf{q})(-\partial_\tau^2 + c^2q^2 + r)\varphi_i(\tau,\mathbf{q}),\\
\mathcal{L}_{\psi-\varphi} &= \lambda\sum_{n=1}^{N}\sum_{\mathbf{k}\,\mathbf{q}} \psi_n^\dagger(\tau,\mathbf{k}+\mathbf{q})\gamma_i\psi_n(\tau,\mathbf{k})\varphi_i(\tau,\mathbf{q}).
\end{aligned} \tag{1}$$

The first term describes N Dirac points and contains the Hermitian γ matrices $\gamma_0 = \sigma_x \otimes s_0$ and $\gamma_i = \sigma_y \otimes s_i$ ($i = x, y, z$), where σ_i (s_i) are Pauli matrices in orbital (spin) space, and σ_0 and s_0 are the identity matrix. While $N = 4$ in cubic systems such as PbTe, we consider the formal limit $N \gg 1$ to neglect vertex corrections in our calculations. The second term describes the propagating transverse optical phonons, with c denoting the phonon velocity and r being the bare phonon mass. Note that $r = 0$ marks the bare FE QCP [52]. Finally, the last term contains the coupling constant λ between the Dirac electrons and the transverse optical phonons.

Tendency to FDW order.—In the normal state, the coupling to the Dirac electrons leads to a renormalization of the phonon spectrum encoded in the polarization operator

$$\Pi_n^{ij}(i\Omega,\mathbf{q}) = \tilde{\lambda}^2\alpha^2(v_F^2q^2 - \Omega^2)\ln\frac{v_F\Lambda_0 e^{1/3}}{\sqrt{v_F^2q^2+\Omega^2}}P^{ij}(\mathbf{q}), \tag{2}$$

where $\tilde{\lambda}^2 \equiv \lambda^2 N/12\pi^2 v_F c^2$, $\alpha \equiv c/v_F$ is the velocity ratio, and Λ_0 is the high-momentum cutoff. We assume throughout this Letter that the effective coupling constant is small, $\tilde{\lambda} \ll 1$, and that Fermi velocity is much larger than the bare transverse phonon velocity, $\alpha \ll 1$. The effective normal state phonon propagator is then given by $\hat{D}_n^{-1} = \hat{D}_0^{-1} - \hat{\Pi}_n$, where $(D_0^{-1})_{ij}(i\Omega,\mathbf{q}) = (r + c^2q^2 + \Omega^2)P_{ij}(\mathbf{q})$ is the bare propagator [53]. Minimization with respect to momentum reveals that, due to the logarithmic dependence in Eq. (2), the original $q = 0$ FE transition is preempted by one at a finite momentum $|\mathbf{q}| = Q$, where

$$Q = \Lambda_0\exp\left(-\frac{1}{\tilde{\lambda}^2} - \frac{1}{6}\right), \tag{3}$$

and the static polarization is transverse. Near the minimum $q = Q$, the static bosonic propagator can be expanded as

$$D_n^{-1}(0,q) \approx r - r_{\mathrm{FDW}} + \tilde{\lambda}^2c^2(q-Q)^2, \tag{4}$$

where $r_{\mathrm{FDW}} = \tilde{\lambda}^2c^2Q^2/2$. We note that Q is exactly the scale appearing in the RG equations derived in Ref. [8] where the system reaches the strong-coupling regime. Equation (4) has a minimum on the whole sphere $q = Q$ instead of a single point at $q = 0$ implying more phase space for fluctuations. Bosonic models of this type are known to undergo a weak fluctuation-driven first-order transition [54,55], which we will neglect hereafter.

Synergistic FDW and SC orders.—We proceed to discuss the possibility of a pairing instability near the emergent FDW QCP by solving the coupled Eliashberg equations [56] inside the paraelectric (PE) phase at the temperature $T = 0$. First, we analytically solve the equations in a BCS-like approximation which implies neglecting the electronic normal self-energy as well as the frequency and momentum dependence of the superconducting order parameter Δ. The boson self-energy $\Pi(i\Omega, q, \Delta)$, however, is computed fully self-consistently. Then, we compare our analytic result with a numerical solution of the frequency-dependent Eliashberg equations and find good qualitative agreement. As we shall shortly detail, we find a range of the parameter r, where the gap equation has a nontrivial solution $\Delta = \Delta_*(r) \neq 0$ in spite of the vanishing density of states. However, by analyzing the free energy in the vicinity of this solution, we show that Δ_* is in fact an unstable solution, which indicates the existence of a stable minimum where the system develops both FDW and SC orders simultaneously through a first-order phase transition.

The mechanism driving the first-order transition stems from the feedback of the SC gap Δ on the boson propagator $D(i\Omega, q, \Delta)$. For $\Delta = 0$, the one-loop polarization operator is given by Eq. (2) and the minimum of D^{-1} is at the finite momentum $q = Q$, Eq. (3). The introduction of a finite (constant) Δ has two important effects on $D^{-1}(i\Omega, \mathbf{q}, \Delta)$

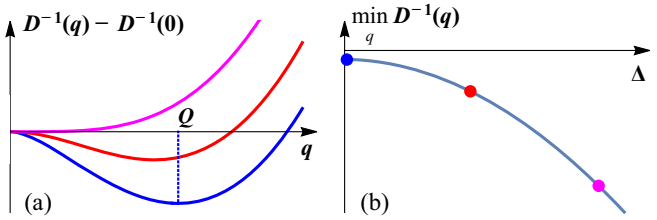

FIG. 1. (a) Inverse static phonon propagator $D^{-1}(q)$, which is proportional to the inverse pairing interaction, as a function of momentum for fixed r and $\Delta/\Delta_0 = 0$ (blue), 0.5 (red), and 1 (purple), with Δ_0 given by Eq. (5). $D^{-1}(q = 0)$ was subtracted for better visualization. (b) The minimal value of D^{-1} shifts to lower values with increasing Δ, signaling a decrease in the spectral mass $m^2(r, \Delta)$ from Eq. (9).

[56], which we illustrate in Fig. 1. First, the position of the minimum gradually shifts toward smaller q until it merges with the $q = 0$ local maximum at Δ_0 given by

$$\Delta_0 = \exp(-5/6) v_F Q. \tag{5}$$

When $\Delta > \Delta_0$, the minimum of D^{-1} shifts back to $q = 0$. Second, a finite Δ reduces the value of the global minimum of D^{-1}, as shown in Fig. 1(b). Thus, increasing Δ makes the FDW mode softer, which in turn increases the pairing interaction. This scenario should be contrasted with other models for superconductivity in the vicinity of a QCP, where the SC order and the order associated with the QCP generally compete, see, e.g., Refs. [46–49]. Here, the two long-range ordered states not only mutually enhance each other, but they are also characterized by the same energy scale $v_F Q$.

Gap equation.—We now discuss the solutions of the gap equation when approaching the FDW QCP from the PE side, focusing on the leading s-wave channel [63,64]:

$$\Delta = \frac{6\tilde{\lambda}^2 \alpha^2 v_F^3}{\pi N} \int_{-\infty}^{\infty} d\omega \int_0^{\Lambda_0} dk k^2 \frac{\Delta \cdot D(i\omega, k, \Delta)}{\omega^2 + v_F^2 k^2 + \Delta^2}. \tag{6}$$

Note that D plays the role of an effective pairing interaction, and that this equation always has the trivial solution $\Delta = 0$. Furthermore, this equation admits a nontrivial solution because the integral gives a Cooper-like logarithm. The one-dimensional nature of this logarithm, however, does not arise from the electron's propagator having a finite chemical potential, but instead from the phonon's propagator being peaked at a finite momentum [56]. If we neglect the feedback of Δ on D discussed above, we find a "standard" instability toward pairing peaked at the FDW QCP. As shown by the red dashed line in Fig. 2, in this case Δ diverges at the QCP $r = r_{\mathrm{FDW}}$. However, upon including Δ self-consistently in D, the situation changes dramatically. Indeed, solving Eq. (6) reveals three important ranges of r. In the immediate vicinity of the putative FDW QCP, $r_{\mathrm{FDW}} < r \leq r_1$, the only solution we find is $\Delta = 0$. The

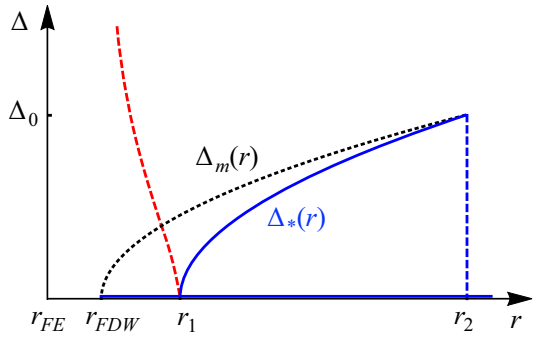

FIG. 2. Nontrivial superconducting solution Δ_* (blue line) as a function of the tuning parameter r. The red dashed line represents the "superconducting dome" one would obtain by ignoring the feedback effect of the SC gap Δ on the phonon propagator D. The values of Δ_0, r_{FDW}, r_1, and r_2 are defined in the main text. The black dotted line shows $\Delta_m(r)$ defined below Eq. (9). The exponentially small region $r_{\mathrm{FDW}} < r < r_1$ was inflated for illustrative purposes.

first nontrivial solution Δ_* appears at $r_1 = r_{\mathrm{FDW}} + \delta r$, where

$$\delta r \sim \tilde{\lambda}^2 c^2 Q^2 \exp\left(-\frac{N\sqrt{1+\alpha^2}}{6\tilde{\lambda}\alpha} + \frac{2}{\tilde{\lambda}}\right). \tag{7}$$

The value of Δ_* increases as we move further away from the QCP, $r_1 < r < r_2$, until it reaches the value $\Delta_* = \Delta_0$ given by Eq. (5) at $r = r_2$:

$$r_2 = 6e^{-5/3}\left(1 + \frac{\tilde{\lambda}^2}{2}\right) c^2 Q^2. \tag{8}$$

Finally, the nontrivial solution disappears abruptly for $r \geq r_2$ provided that $12\alpha/N \lesssim 1$. The full dependence of the solution $\Delta_*(r)$ on the tuning parameter r is shown in Fig. 2 by the solid blue curve. Note, however, that the region $r_{\mathrm{FDW}} < r < r_1$ is exponentially small even on the scale of the exponentially small $v_F Q$.

To confirm that these results are not an artifact of the BCS approximation, we also numerically solve the coupled Eliashberg equations with full frequency dependence of the gap function and including the normal part of the electron's self-energy [56]. Overall, we find the same qualitative behavior of a nontrivial solution that grows upon increasing r away from r_{FDW}. The main impact of the normal part of the self-energy is a reduction in the value of Δ_*.

First-order transition into an FDW + SC *state.*—The increase of the nontrivial solution $\Delta_*(r)$ upon moving away from the QCP in the range $r_1 < r < r_2$ seems at odds with the naive expectation that superconductivity is maximal at the QCP, or at least grows upon approaching it. To understand this, we analyze the superconducting free energy $F[\Delta]$. Expressing the gap equation (6) as $1 = f[\Delta_*]$, the free energy derivative can be conveniently written as

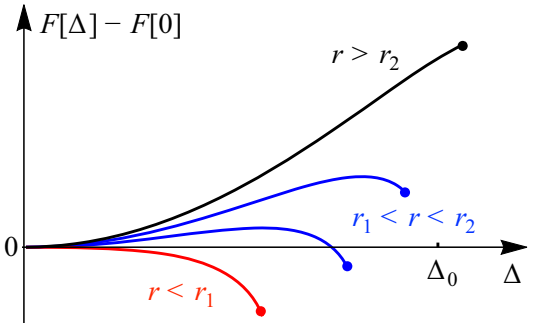

FIG. 3. Superconducting free energy $F[\Delta]$ for different fixed values of the tuning parameter r in the PE phase. The red curve with a maximum at $\Delta = 0$ is from the region $r_{\mathrm{FDW}} < r < r_1$. The blue curves are from the region $r_1 < r < r_2$ and exhibit a local minimum at $\Delta = 0$ and a local maximum at $0 < \Delta_* < \Delta_0$. The black curve with $r > r_2$ has a single minimum at $\Delta = 0$. All curves end at the points where the corresponding spectral mass $m^2(r, \Delta)$ vanishes (bold dots), i.e., at $\Delta_m(r)$, which indicates an instability toward the FDW state.

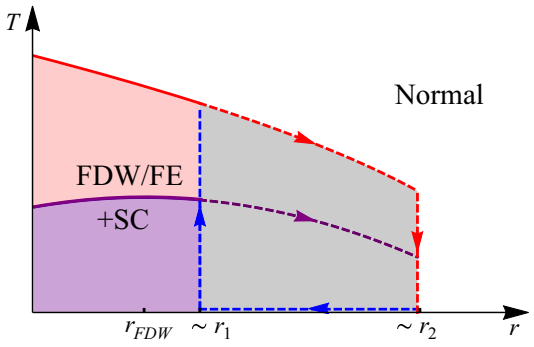

FIG. 4. The expected phase diagram showing the interplay between the FDW/FE and SC orders. The two ordered states enhance each other upon approaching the bare critical point r_{FDW}, resulting in a first-order transition into the state where FDW/FE and SC coexist. The transition is accompanied by the characteristic bistable region with two local energy minima (gray region). "Normal" marks the nonsuperconducting paraelectric region.

$\partial F[\Delta]/\partial\Delta = \Delta - \Delta f[\Delta]$. Because $\partial f/\partial\Delta > 0$ at $\Delta = \Delta_*$ (as can be understood from the dependence of D on Δ shown in Fig. 1), it follows that $\partial^2 F/\partial\Delta^2 < 0$ at $\Delta = \Delta_*$, i.e., the nontrivial solution is *unstable* [56]. The fact that Δ_* is a local maximum of the free energy is further illustrated in Fig. 3, where $F[\Delta]$ is plotted as a function of Δ for different fixed values of r. This situation should be contrasted with the standard BCS gap equation for a Fermi liquid with attractive interactions, where the nontrivial solution is always a local minimum of the free energy.

To understand the relationship between the SC and FDW order parameters, we introduce the phonon spectral mass:

$$m^2(r, \Delta) \equiv \min_q D^{-1}(0, q, \Delta, r). \tag{9}$$

The PE phase corresponds to $m^2(r, \Delta) > 0$, while $m^2(r, \Delta) < 0$ indicates the structural instability toward FDW order. The equation $m^2(r, \Delta_m) = 0$ defines the threshold gap value $\Delta_m(r)$ above which the PE-superconducting system is unstable toward the development of FDW order in conjunction with superconductivity for a given r. These values correspond to the termination points of the free energy curves in Fig. 3. The curve $\Delta_m(r)$ is shown by the black dotted line in Fig. 2, with $\Delta_m(r_{\mathrm{FDW}}) = 0$ and $\Delta_m(r_2) = \Delta_0$.

We thus conclude that the solution $\Delta_*(r)$ is an instability line separating the two stable solutions: (i) a trivial $\Delta = 0$ solution and (ii) a second nontrivial solution $\Delta > \Delta_m(r)$ inside the FDW phase, which cannot be accessed by our gap equation derived in the PE phase. For $r \le r_1$, the trivial solution $\Delta = 0$ is unstable and superconductivity becomes inevitable. We note that we cannot determine whether the ordered state has uniform FE or modulated FDW order, since our analysis is done on the PE side of the transition. Nonetheless, we refer to the ordered state as FDW for definiteness.

The shape of the free energy landscape in Fig. 3 is typical of a system undergoing a first-order transition, as it displays two local minima [one at $\Delta = 0$ and another at $\Delta > \Delta_m(r)$] and one local maximum at $0 < \Delta_*(r) < \Delta_m(r)$ for $r_1 < r < r_2$. This behavior is rooted in the unusual positive feedback effect of a gap opening on the effective pairing interaction D of Eq. (6) [65]. This feedback is stabilized only when FDW order sets in, signaling a coexistence between SC and FDW orders. This also explains the absence of a nontrivial solution $\Delta_*(r)$ for $r > r_2$, since in this range the line $\Delta_*(r)$ is above $\Delta_m(r)$, which means that the system must already be in the FDW phase.

The expected first-order phase diagram emerging from this analysis is shown schematically in Fig. 4. Upon approaching the FE QCP from large values of r, the system can remain in the non-SC and PE state, which is locally stable. At some point $r \ge r_1$, Δ jumps to a finite value and the system undergoes a first-order transition into the state where SC and FDW coexist. On the other hand, upon increasing r from the FDW side ($r < r_{\mathrm{FDW}}$), the system is already SC, and therefore, can remain in this locally stable minimum until some larger value of r is reached, where Δ jumps abruptly to zero and the system becomes PE. A detailed calculation of the Ginzburg-Landau free energy in the ordered FDW state, which is needed to determine precisely the global free-energy minimum, is outside the scope of this Letter. Note also that our approach is justified as long as the first-order simultaneous SC + FDW transition happens before the fluctuation-driven weakly first-order transition expected for the purely bosonic FDW propagator of Eq. (4).

In order for the superconducting state discussed above to be stable against phase fluctuations, it must have a finite

superfluid stiffness ρ_s. In a BCS superconductor, ρ_s is proportional to the electronic density. In the case of a Dirac semimetal at charge neutrality, we find that the gap itself generates an emergent density scale $(\Delta/v_F)^3$, which leads to a finite stiffness despite the vanishing density of states. In the uniform FE phase, we find

$$\rho_s \sim \frac{e^2}{v_F}\Delta^2 \ln\left(\frac{v_F\Lambda_0}{\Delta}\right). \tag{10}$$

We expect this result to hold inside the FDW phase as well. The finite stiffness even at charge neutrality originates from the charge reservoir provided by the filled valence band [66].

Discussion.—We have found that the strong coupling between a FE QCP and a charge neutral Dirac point [8] leads to the first-order transition into the state where nonuniform ferroelectric order and superconductivity appear simultaneously. The key ingredients crucial for this result are the Dirac band touching and its linear coupling to the inversion-odd transverse critical modes.

Our low-energy model of a Dirac semimetal near a putative QCP is possibly relevant to the alloy $Pb_xSn_{1-x}Te$. SnTe ($x = 0$) is a ferroelectric crystalline topological insulator [67]. PbTe ($x = 1$), on the other hand, is a paraelectric and higher order topological insulator [68]. For intermediate x, a ferroelectric-paraelectric transition takes place at $x \approx 0.5$ [69,70]. Doping this composition with indium promotes superconductivity, and is accompanied by unusual features in the phonon density of states [31,32,71]. Using experimental parameters for PbTe we estimate the effective coupling constant to be $\tilde{\lambda}^2 \approx 0.27$ [56]. Thus, we predict the possibility of nonuniform ferroelectricity and low density superconductivity in the alloy $(Pb_{1-x}Sn_x)_{1-y}In_yTe$.

The onset of an FDW phase in this compound should lead to translational symmetry breaking, which could be experimentally detected in the lattice degrees of freedom by neutron and Raman spectroscopy, and in the electronic degrees of freedom by angle-resolved photoemission spectroscopy and quantum oscillations [72].

Furthermore, our results raise a number of questions. The first challenge is to perform a complimentary study on the ordered side of the transition. Second, the phenomenological nature of the zero density superconductor calls for research, e.g., the nature of its collective modes. Also, studying the influence of disorder on the coupled transition is critical in making connection to real materials. Finally, understanding how the phase diagram depends on chemical potential may help make connection to ferroelectric metals with a Fermi surface. For instance, in the case of a Fermi liquid near a putative dipolar ferromagnetic QCP (rather than our dipolar ferroelectric QCP), it is well established that an instability toward a finite-momentum magnetic state is driven by quantum fluctuations [73–75].

We acknowledge helpful discussions with A. Chubukov, M. Gastiasoro, D. Maslov, and T. Trevisan. V. K. was supported by the Quantum Materials program at LBNL, funded by the U.S. Department of Energy under Contract No. DE-AC02-05CH11231. Work by A. K. (while at the University of Minnesota) and R. M. F. was supported by the U.S. Department of Energy through the University of Minnesota Center for Quantum Materials, under Grant No. DE-SC-0016371. The final stage of the work by A. K. and J. R. was supported by the Israel Science Foundation (ISF), and the Directorate for Defense Research and Development (DDR&D), Grant No. 3467/21. The final stage of the work by V. K. was performed in part at Aspen Center for Physics, which is supported by National Science Foundation Grant No. PHY-1607611 and by a grant from the Simons Foundation.

[1] J. F. Schooley, W. R. Hosler, and Marvin L. Cohen, Superconductivity in Semiconducting $SrTiO_3$, Phys. Rev. Lett. **12**, 474 (1964).
[2] Xiao Lin, German Bridoux, Adrien Gourgout, Gabriel Seyfarth, Steffen Krämer, Marc Nardone, Benoît Fauqué, and Kamran Behnia, Critical Doping for the Onset of a Two-Band Superconducting Ground State in $SrTiO_{3-\delta}$, Phys. Rev. Lett. **112**, 207002 (2014).
[3] Terence M. Bretz-Sullivan, Alexander Edelman, J. S. Jiang, Alexey Suslov, David Graf, Jianjie Zhang, Gensheng Wang, Clarence Chang, John E. Pearson, Alex B. Martinson, Peter B. Littlewood, and Anand Bhattacharya, Superconductivity in the dilute single band limit in reduced strontium titanate, arXiv:1904.03121.
[4] Zhongheng Liu, Xiong Yao, Jifeng Shao, Ming Zuo, Li Pi, Shun Tan, Changjin Zhang, and Yuheng Zhang, Superconductivity with topological surface state in $Sr_xBi_2Se_3$, J. Am. Chem. Soc. **137**, 10512 (2015).
[5] N. P. Butch, P. Syers, K. Kirshenbaum, A. P. Hope, and J. Paglione, Superconductivity in the topological semimetal YPtBi, Phys. Rev. B **84**, 220504(R) (2011).
[6] Y. Matsushita, P. A. Wianecki, A. T. Sommer, T. H. Geballe, and I. R. Fisher, Type II superconducting parameters of Tl-doped PbTe determined from heat capacity and electronic transport measurements, Phys. Rev. B **74**, 134512 (2006).
[7] Om Prakash, Anil Kumar, A. Thamizhavel, and S. Ramakrishnan, Evidence for bulk superconductivity in pure bismuth single crystals at ambient pressure, Science **355**, 52 (2017).
[8] Vladyslav Kozii, Zhen Bi, and Jonathan Ruhman, Superconductivity near a Ferroelectric Quantum Critical Point in Ultralow-Density Dirac Materials, Phys. Rev. X **9**, 031046 (2019).
[9] Maria N. Gastiasoro, Jonathan Ruhman, and Rafael M. Fernandes, Superconductivity in dilute $SrTiO_3$: A review, Ann. Phys. (Amsterdam) **417**, 168107 (2020).
[10] V. L. Gurevich, A. I. Larkin, and Yu. A. Firsov, On the possibility of superconductivity in semiconductors, Sov. Phys. Solid State **4**, 131 (1962).

[11] Maria N. Gastiasoro, Andrey V. Chubukov, and Rafael M. Fernandes, Phonon-mediated superconductivity in low carrier-density systems, Phys. Rev. B **99**, 094524 (2019).

[12] Maria N. Gastiasoro, Thaís V. Trevisan, and Rafael M. Fernandes, Anisotropic superconductivity mediated by ferroelectric fluctuations in cubic systems with spin-orbit coupling, Phys. Rev. B **101**, 174501 (2020).

[13] Andrey V. Chubukov and Jörg Schmalian, Superconductivity due to massless boson exchange in the strong-coupling limit, Phys. Rev. B **72**, 174520 (2005).

[14] S. Lederer, Y. Schattner, E. Berg, and S. A. Kivelson, Enhancement of Superconductivity near a Nematic Quantum Critical Point, Phys. Rev. Lett. **114**, 097001 (2015).

[15] Max A. Metlitski, David F. Mross, Subir Sachdev, and T. Senthil, Cooper pairing in non-Fermi liquids, Phys. Rev. B **91**, 115111 (2015).

[16] Yuxuan Wang, Artem Abanov, Boris L. Altshuler, Emil A. Yuzbashyan, and Andrey V. Chubukov, Superconductivity near a Quantum-Critical Point: The Special Role of the First Matsubara Frequency, Phys. Rev. Lett. **117**, 157001 (2016).

[17] S. E. Rowley, L. J. Spalek, R. P. Smith, M. P. M. Dean, M. Itoh, J. F. Scott, G. G. Lonzarich, and S. S. Saxena, Ferroelectric quantum criticality, Nat. Phys. **10**, 367 (2014).

[18] Jonathan M. Edge, Yaron Kedem, Ulrich Aschauer, Nicola A. Spaldin, and Alexander V. Balatsky, Quantum Critical Origin of the Superconducting Dome in $SrTiO_3$, Phys. Rev. Lett. **115**, 247002 (2015).

[19] Peter Wölfle and Alexander V. Balatsky, Superconductivity at low density near a ferroelectric quantum critical point: Doped $SrTiO_3$, Phys. Rev. B **98**, 104505 (2018).

[20] Yaron Kedem, Novel pairing mechanism for superconductivity at a vanishing level of doping driven by critical ferroelectric modes, Phys. Rev. B **98**, 220505(R) (2018).

[21] Shota Kanasugi and Youichi Yanase, Spin-orbit-coupled ferroelectric superconductivity, Phys. Rev. B **98**, 024521 (2018).

[22] J. R. Arce-Gamboa and G. G. Guzmán-Verri, Quantum ferroelectric instabilities in superconducting $SrTiO_3$, Phys. Rev. Mater. **2**, 104804 (2018).

[23] Carl Willem Rischau, Xiao Lin, Christoph P. Grams, Dennis Finck, Steffen Harms, Johannes Engelmayer, Thomas Lorenz, Yann Gallais, Benoît Fauqué, Joachim Hemberger, and Kamran Behnia, A ferroelectric quantum phase transition inside the superconducting dome of $Sr_{1-x}Ca_xTiO_{3-\delta}$, Nat. Phys. **13**, 643 (2017).

[24] Yasuhide Tomioka, Naoki Shirakawa, Keisuke Shibuya, and Isao H. Inoue, Enhanced superconductivity close to a non-magnetic quantum critical point in electron-doped strontium titanate, Nat. Commun. **10**, 738 (2019).

[25] C. Enderlein, J. Ferreira de Oliveira, D. A. Tompsett, E. Baggio Saitovitch, S. S. Saxena, G. G. Lonzarich, and S. E. Rowley, Superconductivity mediated by polar modes in ferroelectric metals, Nat. Commun. **11**, 4852 (2020).

[26] A. Stucky, G. W. Scheerer, Z. Ren, D. Jaccard, J.-M. Poumirol, C. Barreteau, E. Giannini, and D. van der Marel, Isotope effect in superconducting *n*-doped $SrTiO_3$, Sci. Rep. **6**, 37582 (2016).

[27] Hideaki Sakai, Koji Ikeura, Mohammad Saeed Bahramy, Naoki Ogawa, Daisuke Hashizume, Jun Fujioka, Yoshinori Tokura, and Shintaro Ishiwata, Critical enhancement of thermopower in a chemically tuned polar semimetal $MoTe_2$, Sci. Adv. **2**, e1601378 (2016).

[28] Chloe Herrera, Jonah Cerbin, Amani Jayakody, Kirsty Dunnett, Alexander V. Balatsky, and Ilya Sochnikov, Strain-engineered interaction of quantum polar and superconducting phases, Phys. Rev. Mater. **3**, 124801 (2019).

[29] Johannes Engelmayer, Xiao Lin, and Fulya Koç, Christoph P. Grams, Joachim Hemberger, Kamran Behnia, and Thomas Lorenz, Ferroelectric order versus metallicity in $Sr_{1-x}Ca_xTiO_{3-\delta}$ ($x = 0.009$), Phys. Rev. B **100**, 195121 (2019).

[30] Jialu Wang, Liangwei Yang, Carl Willem Rischau, Zhuokai Xu, Zhi Ren, Thomas Lorenz, Joachim Hemberger, Xiao Lin, and Kamran Behnia, Charge transport in a polar metal, npj Quantum Mater. **4**, 1 (2019).

[31] A. Sapkota, Y. Li, B. L. Winn, A. Podlesnyak, Guangyong Xu, Zhijun Xu, Kejing Ran, Tong Chen, Jian Sun, Jinsheng Wen, Lihua Wu, Jihui Yang, Qiang Li, G. D. Gu, and J. M. Tranquada, Electron-phonon coupling and superconductivity in the doped topological crystalline insulator $(Pb_{0.5}Sn_{0.5})_{1-x}In_xTe$, Phys. Rev. B **102**, 104511 (2020).

[32] R. V. Parfen'ev, D. V. Shamshur, and S. A. Nemov, Superconductivity of $(Sn_{1-z}Pb_z)_{1-x}In_xTe$ alloys, Phys. Solid State **43**, 1845 (2001).

[33] Jonathan Ruhman and Patrick A. Lee, Comment on "Superconductivity at low density near a ferroelectric quantum critical point: Doped $SrTiO_3$, Phys. Rev. B **100**, 226501 (2019).

[34] K. L. Ngai, Two-Phonon Deformation Potential and Superconductivity in Degenerate Semiconductors, Phys. Rev. Lett. **32**, 215 (1974).

[35] D. van der Marel, F. Barantani, and C. W. Rischau, Possible mechanism for superconductivity in doped $SrTiO_3$, Phys. Rev. Res. **1**, 013003 (2019).

[36] Abhishek Kumar, Vladimir I. Yudson, and Dmitrii L. Maslov, Quasiparticle and Nonquasiparticle Transport in Doped Quantum Paraelectrics, Phys. Rev. Lett. **126**, 076601 (2021).

[37] Pavel A. Volkov, Premala Chandra, and Piers Coleman, Superconductivity from energy fluctuations in dilute quantum critical polar metals, Nat. Commun. **13**, 4599 (2022).

[38] Dmitry E. Kiselov and Mikhail V. Feigel'man, Theory of superconductivity due to Ngai's mechanism in lightly doped $SrTiO_3$, Phys. Rev. B **104**, L220506 (2021).

[39] Vladimir I. Fal'ko and Boris N. Narozhny, Triplet pairing due to spin-orbit-assisted electron-phonon coupling, Phys. Rev. B **74**, 012501 (2006).

[40] Liang Fu, Parity-Breaking Phases of Spin-Orbit-Coupled Metals with Gyrotropic, Ferroelectric, and Multipolar Orders, Phys. Rev. Lett. **115**, 026401 (2015).

[41] Vladyslav Kozii and Liang Fu, Odd-Parity Superconductivity in the Vicinity of Inversion Symmetry Breaking in Spin-Orbit-Coupled Systems, Phys. Rev. Lett. **115**, 207002 (2015).

[42] Jonathan Ruhman, Vladyslav Kozii, and Liang Fu, Odd-Parity Superconductivity near an Inversion Breaking Quantum Critical Point in One Dimension, Phys. Rev. Lett. **118**, 227001 (2017).

[43] Fengcheng Wu and Ivar Martin, Nematic and chiral superconductivity induced by odd-parity fluctuations, Phys. Rev. B **96**, 144504 (2017).

[44] Pavel A. Volkov and Premala Chandra, Multiband Quantum Criticality of Polar Metals, Phys. Rev. Lett. **124**, 237601 (2020).

[45] Maria N. Gastiasoro, Maria Eleonora Temperini, Paolo Barone, and Jose Lorenzana, Theory of superconductivity mediated by Rashba coupling in incipient ferroelectrics, Phys. Rev. B **105**, 224503 (2022).

[46] C. A. Balseiro and L. M. Falicov, Superconductivity and charge-density waves, Phys. Rev. B **20**, 4457 (1979).

[47] Tanmoy Das, R. S. Markiewicz, and A. Bansil, Nonmonotonic $d_{x^2-y^2}$ superconducting gap in electron-doped $Pr_{0.89}LaCe_{0.11}CuO_4$: Evidence of coexisting antiferromagnetism and superconductivity?, Phys. Rev. B **74**, 020506(R) (2006).

[48] A. B. Vorontsov, M. G. Vavilov, and A. V. Chubukov, Superconductivity and spin-density waves in multiband metals, Phys. Rev. B **81**, 174538 (2010).

[49] Eun-Gook Moon and Subir Sachdev, Competition between superconductivity and nematic order: Anisotropy of superconducting coherence length, Phys. Rev. B **85**, 184511 (2012).

[50] Rafael M. Fernandes and Jörg Schmalian, Competing order and nature of the pairing state in the iron pnictides, Phys. Rev. B **82**, 014521 (2010).

[51] N. W. Ashcroft and N. D. Mermin, *Solid State Physics* (Holt, Rinehart and Winston, New York, 1976).

[52] Note that here we have assumed the mass term is tuned to zero uniformly. By that, we have assumed the system is clean. How mass disorder affects our results is an important question, which is relevant to experiments.

[53] To properly invert the bosonic propagator, one should keep the mass of the longitudinal mode large but finite and set it to infinity only at the end of the calculation.

[54] S. A. Brazovskii, Phase transition of an isotropic system to a nonuniform state, Sov. J. Exp. Theor. Phys. **41**, 85 (1975).

[55] Rafael M. Fernandes, Jörg Schmalian, and Harry Westfahl, Conductivity of electronic liquid-crystalline mesophases, Phys. Rev. B **78**, 184201 (2008).

[56] See Supplemental Material at http://link.aps.org/supplemental/10.1103/PhysRevLett.129.237001 for the details of the analytical and numerical solutions of the Eliashberg equations and the analysis of their stability. It additionally contains Refs. [57–62].

[57] B. A. Assaf, T. Phuphachong, V. V. Volobuev, A. Inhofer, G. Bauer, G. Springholz, L. A. de Vaulchier, and Y. Guldner, Massive and massless Dirac fermions in $Pb_{1-x}Sn_xTe$ topological crystalline insulator probed by magneto-optical absorption, Sci. Rep. **6**, 20323 (2016).

[58] Matthew K Jacobsen, Wei Liu, and Baosheng Li, Sound velocities of PbTe to 14 GPa: Evidence for coupling between acoustic and optic phonons, J. Phys. Condens. Matter **25**, 365402 (2013).

[59] Jiming An, Alaska Subedi, and D. J. Singh, *Ab initio* phonon dispersions for PbTe, Solid State Commun. **148**, 417 (2008).

[60] Y Tanaka, Zhi Ren, T Sato, K Nakayama, S Souma, T Takahashi, Kouji Segawa, and Yoichi Ando, Experimental realization of a topological crystalline insulator in SnTe, Nat. Phys. **8**, 800 (2012).

[61] Chao Yang, Yanyu Liu, Gang Tang, Xueyun Wang, and Jiawang Hong, Non-monotonic thickness dependence of Curie temperature and ferroelectricity in two-dimensional SnTe film, Appl. Phys. Lett. **113**, 082905 (2018).

[62] Yao Wang, Chengcheng Xiao, Miaogen Chen, Chenqiang Hua, Junding Zou, Chen Wu, Jianzhong Jiang, Shengyuan A. Yang, Yunhao Lu, and Wei Ji, Two-dimensional ferroelectricity and switchable spin-textures in ultra-thin elemental Te multilayers, Mater. Horizons **5**, 521 (2018).

[63] P. M. R. Brydon, S. Das Sarma, Hoi-Yin Hui, and Jay D. Sau, Odd-parity superconductivity from phonon-mediated pairing: Application to $Cu_xBi_2Se_3$, Phys. Rev. B **90**, 184512 (2014).

[64] By projecting the interaction in Eq. (1) onto the momentum-independent pairing channels, we find that the only attractive channel is the fully symmetric s wave [56].

[65] Increasing Δ generally has two opposite effects on the boson propagator: (1) it shifts the minimum of D^{-1} toward smaller momenta q and (2) it decreases the phonon spectral mass. The first effect reduces the strength of the FDW fluctuations while the second one increases it, and our calculation shows that the latter effect is dominant.

[66] Andrey V. Chubukov, Ilya Eremin, and Dmitri V. Efremov, Superconductivity versus bound-state formation in a two-band superconductor with small Fermi energy: Applications to Fe pnictides/chalcogenides and doped $SrTiO_3$, Phys. Rev. B **93**, 174516 (2016).

[67] Timothy H Hsieh, Hsin Lin, Junwei Liu, Wenhui Duan, Arun Bansil, and Liang Fu, Topological crystalline insulators in the SnTe material class, Nat. Commun. **3**, 982 (2012).

[68] Iñigo Robredo, Maia G. Vergniory, and Barry Bradlyn, Higher-order and crystalline topology in a phenomenological tight-binding model of lead telluride, Phys. Rev. Mater. **3**, 041202(R) (2019).

[69] W. J. Daughton, C. W. Tompson, and E. Gurmen, Lattice instability and phonon lifetimes in $Pb_{1-x}Sn_xTe$ alloys, J. Phys. C **11**, 1573 (1978).

[70] H. Bilz, A. Bussmann-Holder, W. Jantsch, and P. Vogl, *Dynamical Properties of IV-VI Compounds*, Springer Tracts in Modern Physics Vol. 99 (Springer-Verlag, Berlin, Heidelberg, 1983).

[71] Kejing Ran, Ruidan Zhong, Tong Chen, Yuan Gan, Jinghui Wang, B. L. Winn, A. D. Christianson, Shichao Li, Zhen Ma, Song Bao, Zhengwei Cai, Guangyong Xu, J. M. Tranquada, Genda Gu, Jian Sun, and Jinsheng Wen, Unusual phonon density of states and response to the superconducting transition in the In-doped topological crystalline insulator $Pb_{0.5}Sn_{0.5}Te$, Phys. Rev. B **97**, 220502(R) (2018).

[72] Tian Liang, Satya Kushwaha, Jinwoong Kim, Quinn Gibson, Jingjing Lin, Nicholas Kioussis, Robert J. Cava, and N. Phuan Ong, A pressure-induced topological phase with large Berry curvature in $Pb_{1-x}Sn_xTe$, Sci. Adv. **3**, e1602510 (2017).

[73] D. Belitz, T. R. Kirkpatrick, and Thomas Vojta, Nonanalytic behavior of the spin susceptibility in clean Fermi systems, Phys. Rev. B **55**, 9452 (1997).

[74] Dmitrii L. Maslov and Andrey V. Chubukov, Nonanalytic paramagnetic response of itinerant fermions away and near a ferromagnetic quantum phase transition, Phys. Rev. B **79**, 075112 (2009).

[75] Andrew G. Green, Gareth Conduit, and Frank Krüger, Quantum order-by-disorder in strongly correlated metals, Annu. Rev. Condens. Matter Phys. **9**, 59 (2018).